part properties of the macrocycle and anion solvation spheres rather than specific properties of the complexing ions. This formulation also provides a rationale for the anion complexation reactions of highly protonated macrocycle species while such reactions have not been observed with apparently similar linear polyamines. That is, the linear structures do not assemble a sufficiently large solvation sphere, which by its subsequent partial dispersal provides the driving force for anion complexation.

Registry No. $H_4L(SO_4)_2$, 101031-39-4.

Contribution from the Departments of Chemistry, University of Michigan, Ann Arbor, Michigan 48109, Oakland University, Rochester, Michigan 48063, and University of Helsinki, Et. Hesperiankatu 4, 00100 Helsinki, Finland

Multinuclear NMR Characterization of Anionic Clusters of the Main-Group Elements Ge, Sn, Sb, Tl, Pb, and Bi in Nonaqueous Solution

William L. Wilson,[†1] Ralph W. Rudolph,[†2] Lawrence L. Lohr,[*†] R. Craig Taylor,[‡] and Pekka Pyykkö[§]

Received September 7, 1984

Anionic clusters of the elements Ge, Sn, Sb, Tl, Pb, and Bi have been generated by dissolving their alloys with alkali metals in liquid ethylenediamine. The clusters have been identified by ^{119}Sn, ^{205}Tl, and ^{207}Pb NMR techniques. Spin–spin coupling constants (^{119}Sn–^{117}Sn, ^{119}Sn–^{203,205}Tl, and ^{119}Sn–^{207}Pb) and chemical shifts (^{119}Sn and ^{207}Pb) are presented for a large number of clusters with a range of alkali-metal cations. Clusters not previously reported include $Sn_{8-x}Pb_xTl^{n-}$ (x = 1–4, n probably 5); $Sn_2Bi_2^{2-}$ is characterized in solution for the first time. A number of systematic trends in the data are presented and discussed. The origins of the spin–spin couplings are discussed in terms of the relativistic theory of the coupling with the aid of relativistically parametrized (REX) semiempirical molecular orbital calculations.

I. Introduction

A large number of anionic clusters of group 3B–5B (13–15)[49] elements have been generated by the extraction of Zintl alloylike phases with nonaqueous solvents such as ethylenediamine (en) or ammonia and characterized[3-8] by ^{119}Sn, ^{205}Tl, or ^{207}Pb NMR spectroscopy. Clusters that have been identified include $Sn_{9-x}Pb_x^{4-}$ (x = 0–9),[4,5] $Sn_{9-x}Ge_x^{4-}$ (x = 0–9),[6] Sn_8Tl^{5-},[6] Sn_4^{2-},[6] $SnTe_4^{4-}$,[6] $Sn_9ML_2^{4-}$, and $Sn_8TlML_2^{5-}$ (M = Pd, Pt; L_2 = en).[7,8] The list of clusters is similar to that of anionic clusters which have been isolated from solution as salts of alkali metals complexed with the bicyclic 2,2,2-crypt ligand. These include Sb_4^{2-} and Sb_7^{3-},[9,10] Te_3^{2-},[11] Bi_4^{2-},[12] Sn_5^{2-} and Pb_5^{2-},[13] Sn_9^{4-},[14] Ge_9^{4-} and Ge_9^{2-},[15] As_{11}^{2-},[16] $Tl_2Te_2^{2-}$,[17] $Sn_2Bi_2^{2-}$,[18] Sn_xTl^{3-} (x = 8, 9),[19] $HgTe_2^{2-}$,[20] and Sn_9^{3-}.[21] Closely related are the large number of known cationic clusters,[22] including Bi_5^{3+},[23] Bi_8^{2+},[24] Bi_9^{5+},[23-25] Se_8^{2+},[27] $Te_{4-x}Se_x^{2+}$ (x = 0–4),[28-31] $Te_{6-x}Se_x^{2+}$ (x = 0, 3, 4),[32] and Se_{10}^{2+}.[33] A key observation[3-8] from ^{119}Sn NMR of solutions of anionic clusters containing Sn is a single ^{119}Sn chemical shift δ and a single ^{119}Sn–^{117}Sn coupling constant for a given cluster, from which it is concluded[3-6] that clusters such as $Sn_{9-x}M_x^{4-}$ (M = Ge, Pb) are fluxional.

We report here for the first time the identification by NMR in solution of the clusters $Sn_{8-x}Pb_xTl^{5-}$ (x = 1–4) and $Sn_2Bi_2^{2-}$. We also present a compilation of ^{119}Sn and ^{207}Pb chemical shifts together with ^{119}Sn–^{117}Sn, ^{119}Sn–^{207}Pb, and ^{119}Sn–^{203,205}Tl coupling constants for a large number of nine-atom anionic clusters of the form $Sn_{9-x-y}A_xB_y^{q-}$ (A, B = Ge, Tl, Pb), with the data being presented as a function of the accompanying alkali cation, ranging from Li^+ to Cs^+ in some cases but more typically from Na^+ to Cs^+. Finally, we present a discussion and an interpretation of the nuclear spin–spin coupling constants in terms of the relativistic theory[34] of these couplings.

II. Experimental Section

Table I. Clusters and Alloys from Which They Were Obtained

cluster	alloys[a]
Sn_9^{4-}	LiSn, $LiSn_2$, $NaSn_4$, Na_4Sn_9, $NaSn_2$, NaSn (NH_3, CH_3NH_2), KSn_2, KSn_3
Pb_9^{4-}	KPb_2, $NaPb_2$, $NaPb_3$, Li_4Pb_9, $LiPb_2$
$Sn_{9-x}Pb_x^{4-}$ (x = 0–9)	LiSnPb, NaSnPb, $Na_4Sn_3Pb_6$, $Na_4Sn_6Pb_3$, KSnPb, RbSnPb, CsSnPb
$Sn_{9-x}Ge_x^{4-}$ (x = 0–9)	NaSnGe, KSnGe, K_2SnGe_3, RbSnGe
Sn_8Tl^{5-}	$Na_2Sn_2Tl_3$, $K_2Sn_2Tl_3$
$Sn_{8-x}Pb_xTl^{5-}$ (x = 0–8)	$Na_2SnPbTl_3$, $K_2SnPbTl_3$
$Sn_2Bi_2^{2-}$	LiSnBi, NaSnBi
Sn_4^{2-} [b]	NaSn (en), Na_3Sn_2 (en), Na_2Sn (en), NaSnCu (en)
$SnTe_4^{4-}$ [b]	NaSnTe

[a] Where important, the solvent is listed in parentheses after the alloy. The compositions of the alloys are nominal and are not intended to represent pure phases. [b] Reference 6.

As described in our earlier papers,[4-6] alloys of group 3B–5B elements with alkali metals were prepared by fusion. Typically, the elements were heated in Vycor tubes under N_2 at 0.9 atm (at room temperature) and, after cooling, were extracted with en to form deeply colored solutions (orange-red for Sn_9^{4-}). To minimize contaminations, the extractions were carried out in NMR tubes, each sealed to a stopcock fitted with a ground-glass joint. Extraction times were typically 2–24 h but were 48 h–2 weeks for alloys containing Na. The times were selected to obtain

---

[*] To whom correspondence should be addressed.

[†] University of Michigan.

[‡] Oakland University.

[§] University of Helsinki.

(1) Present address: Department of Chemistry, University of Georgia, Athens, GA 30602.
(2) Deceased May 11, 1981.
(3) Wilson, W. L. Ph.D. Thesis, University of Michigan, Ann Arbor, MI, 1982.
(4) Rudolph, R. W.; Wilson, W. L.; Parker, F.; Taylor, R. C.; Young, D. C. *J. Am. Chem. Soc.* **1978**, *100*, 4629.
(5) Rudolph, R. W.; Taylor, R. C.; Young, D. C. *Fundamental Research in Homogeneous Catalysis*; Tsutsui, M., Ed.; Plenum: New York, 1979; pp 997–1005.
(6) Rudolph, R. W.; Wilson, W. L.; Taylor, R. C. *J. Am. Chem. Soc.* **1981**, *103*, 2480.
(7) Teixidor, F.; Luetkens, M. L., Jr.; Rudolph, R. W. *J. Am. Chem. Soc.* **1983**, *105*, 149.
(8) Luetkens, M. L., Jr.; Teixidor, F.; Rudolph, R. W. *Inorg. Chim. Acta* **1984**, *83*, L13.
(9) Adolphson, D. G.; Corbett, J. D.; Merryman, D. J. *J. Am. Chem. Soc.* **1976**, *98*, 7233.
(10) Critchlow, S. C.; Corbett, J. D. *Inorg. Chem.* **1984**, *23*, 770.
(11) Cisar, A.; Corbett, J. D. *Inorg. Chem.* **1977**, *16*, 632.
(12) Cisar, A.; Corbett, J. D. *Inorg. Chem.* **1977**, *16*, 2482.
(13) Edwards, P. A.; Corbett, J. D. *Inorg. Chem.* **1977**, *16*, 903.
(14) Corbett, J. D.; Edwards, P. A. *J. Am. Chem. Soc.* **1977**, *99*, 3313.
(15) Belin, C. H. E.; Corbett, J. D.; Cisar, A. *J. Am. Chem. Soc.* **1977**, *99*, 7163.
(16) Belin, C. H. E. *J. Am. Chem. Soc.* **1980**, *102*, 6036.
(17) Burns, R. C.; Corbett, J. D. *J. Am. Chem. Soc.* **1981**, *103*, 2627.
(18) Critchlow, S. C.; Corbett, J. D. *Inorg. Chem.* **1982**, *21*, 3286.
(19) Burns, R. C.; Corbett, J. D. *J. Am. Chem. Soc.* **1982**, *104*, 2804.
(20) Burns, R. C.; Corbett, J. D. *Inorg. Chem.* **1981**, *20*, 4433.
(21) Critchlow, S. C.; Corbett, J. D. *J. Am. Chem. Soc.* **1983**, *105*, 5715.

0020-1669/86/1325-1535$01.50/0 © 1986 American Chemical Society

the maximum possible NMR intensity. Table I gives a list of clusters identified in solution of various alloys. In some cases the solutions show additional NMR lines corresponding to unidentified clusters.

NMR data were obtained with Varian FT-80 (Oakland University), JEOL FX-90Q, and Bruker 360 (both at the University of Michigan) spectrometers. The Varian FT-80 spectrometer is equipped with a multinuclear probe and operates at a temperature of 29.0 ± 0.5 °C. All samples were run in sealed 10-mm tubes.

The ^{119}Sn spectra were recorded at either 29.619 or 29.606 MHz with spectral widths of 8 and 16 kHz, respectively. Line widths were typically 5–12 Hz, depending on the sample. With use of the full data table available on the spectrometer, the data point resolution varied from 1 to 2 Hz with acquisition times of 0.5 s. The 90° tip angle for $\text{Sn}_9{}^{4-}$ was measured at 22 s, and since T_1 for this same species was determined to be 0.3–0.5 s by using the inversion recovery technique, pulse widths were chosen to give 45–60° flip angles. Chemical shifts were measured relative to external Me_4Sn (neat).

The ^{207}Pb spectra were recorded at either 16.570 or 16.595 MHz with spectral windows of 8 and 25 kHz, respectively. All other spectral parameters were similar to those used in obtaining the ^{119}Sn spectra. Line widths were measured in the range of 6–8 Hz. Chemical shifts were measured relative to external 1 M $\text{Pb(NO}_3)_2$.

The ^{205}Tl spectra were recorded at 45.903 MHz on a Varian FT-80A spectrometer equipped with a multinuclear probe tunable between 32 and 80 MHz. Acquisition times, pulse widths, spectral windows (8 kHz only), and other instrumental parameters were similar to those used in obtaining ^{119}Sn spectra. Line widths were in the range of 8–12 Hz, depending on the sample. The chemical shifts were measured relative to external 0.1 M $\text{Tl(NO}_3)$.

A minimum of four separate measurements of line widths, chemical shifts, and satellite intensities were made on each sample involving observation of ^{119}Sn and ^{207}Pb spectra. Errors in line widths and chemical shifts were ca. 1–3% on the average. The satellite intensities were accurate to ±1–2% for the $\text{Sn}_{9-x}\text{Pb}^{4-}$ (x = 0–9) and $\text{Sn}_8\text{Tl}^{5-}$ clusters and ±4–5% for the $\text{Sn}_{8-x}\text{Pb}_x\text{Tl}^{5-}$ (x = 1–4) clusters.

III. Species Identification

A. General Considerations. The identification of the species is as previously described;[4–6] namely, the cluster stoichiometry is established from the relative intensity pattern of the spin–spin multiplets in the ^{119}Sn and ^{207}Pb signals. For example, clusters containing eight and nine Sn atoms yield multiplets whose central lines have intensity ratios of 1:0.276:0.033 and 1:0.311:0.044, respectively, so that distinction between these two cluster sizes requires measurement of the relative intensity of the first satellite to an accuracy better than the 15% difference between 0.276 and 0.311. The ^{119}Sn–^{117}Sn coupling constant is taken as the separation between the first high-field and the first low-field satellite. It has proven to be generally satisfactory to base relative intensities on peak heights rather than integrated areas.

The establishment of cluster charges is generally less rigorous than the establishment of cluster stoichiometry. The clusters $\text{Sn}_{9-x}\text{Pb}_x{}^{q-}$ and $\text{Sn}_{9-x}\text{Ge}_x{}^{q-}$ (x = 0–9) were assigned[4–6] the charge 4– in part because salts with the formula $[\text{Na(crypt)}]_4\text{M}_9$ (M = Sn, Ge) have been characterized[14,16] and in part because such a charge assignment ($-{}^4/_9$ per atom) appeared to be more consistent with the observed ^{119}Sn chemical shifts than any other charge assignment. The assignments[4,6] of charges 5– and 3– to the nine-atom clusters containing Tl and Sb, respectively, follow from the assumption of isoelectronic substitutions to Tl^- for Pb and Sb^+ for Sn. An alternative assignment is in some cases possible, so that the cluster assigned as $\text{Sn}_8\text{Tl}^{5-}$ may be $\text{Sn}_8\text{Tl}^{3-}$, as reported[19] for the solid phase. Such an oxidized cluster would be expected to exhibit a much more positive ^{119}Sn chemical shift than the −1169 ppm (with Na^+) value observed. Indeed, the comparatively narrow range of ^{119}Sn values given in Section IV suggests that all of these nine-atom clusters have comparable charge densities about a Sn nucleus, consistent with our charge assignments. The chemical shifts are in no case as negative as the −1895 ppm value assigned[6] to $\text{Sn}_4{}^{2-}$ (with Na^+).

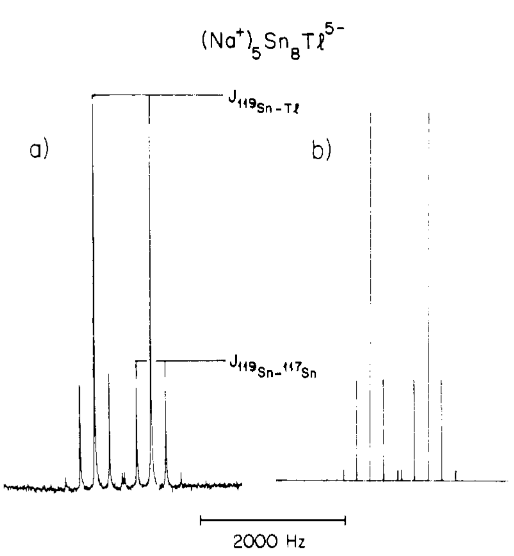

Figure 1. (a) NMR spectrum of ^{119}Sn at 29.8 MHz for $(\text{Na}^+)_5\text{Sn}_8\text{Tl}^{5-}$ in en. (b) Line spectrum calculated for $\text{Sn}_8\text{Tl}^{5-}$ with $J(^{119}\text{Sn}-^{117}\text{Sn})$ = 410 Hz and $J(^{119}\text{Sn}-^{203,205}\text{Tl})$ = 800 Hz. The observed ratios of central to satellite peak heights are 1:0.28:0.034, while the expected intensity ratios for a cluster with eight Sn atoms are 1:0.276:0.033.

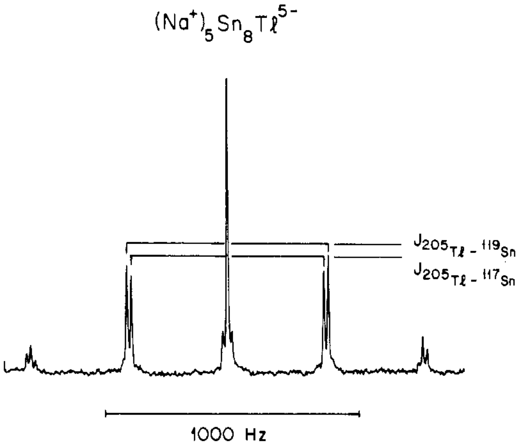

Figure 2. NMR spectrum of ^{205}Tl at 48.0 MHz for $(\text{Na}^+)_5\text{Sn}_8\text{Tl}^{5-}$ in en. Coupling constants are $J(^{205}\text{Tl}-^{119}\text{Sn})$ = 795 Hz and $J(^{205}\text{Tl}-^{117}\text{Sn})$ = 760 Hz. The ratio of satellite peak heights is 0.92, while the expected intensity ratio ($^{117}\text{Sn}/^{119}\text{Sn}$) is 0.906. Other intensity data are given in text.

B. $\text{Sn}_{8-x}\text{Pb}_x\text{Tl}^{5-}$ (x = 0–4). We previously reported[6] the identification of the species $\text{Sn}_8\text{Tl}^{5-}$ from the ^{119}Sn spectrum of the solution of the alloy $\text{Na}_2\text{Sn}_2\text{Tl}_3$ in en. We report here further confirmation of this identification together with evidence for the related clusters $\text{Sn}_{8-x}\text{Pb}_x\text{Tl}^{5-}$ (x = 1–4). In Figures 1 and 2 we show the ^{119}Sn and ^{205}Tl spectra, respectively, for the solution of $\text{Na}_2\text{Sn}_2\text{Tl}_3$ in en. Both spectra indicate a cluster with eight Sn atoms. In Figure 1 the observed ratios of central to satellite peak heights (^{119}Sn–^{117}Sn) are 1:0.28:0.034, while the expected[5] intensity ratios are 1:0.276:0.033. Expected ratios for seven- and nine-Sn clusters are 1:0.239:0.024 and 1:0.311:0.044, respectively. These possibilities appear to be clearly ruled out by the data. The coupling constants are 410 Hz for ^{119}Sn–^{117}Sn and 800 Hz for

---

(22) Corbett, J. D. *Prog. Inorg. Chem.* **1976**, *21*, 129.
(23) Corbett, J. D. *Inorg. Chem.* **1968**, *7*, 198.
(24) Hershaft, A.; Corbett, J. D. *Inorg. Chem.* **1963**, *2*, 979.
(25) Friedman, R. M.; Corbett, J. D. *Inorg. Chim. Acta* **1973**, *7*, 525.
(26) Friedman, R. M.; Corbett, J. D. *Inorg. Chem.* **1973**, *12*, 1134.
(27) McMullan, R. K.; Prince, D. J.; Corbett, J. D. *Inorg. Chem.* **1971**, *10*, 1749.
(28) Brown, I. D.; Crump, D. B.; Gillespie, R. J.; Santry, D. P. *Chem. Commun.* **1968**, 853.
(29) Prince, D. J.; Corbett, J. D.; Garbisch, B. *Inorg. Chem.* **1970**, *9*, 2731.
(30) Couch, T. W.; Lokken, D. A.; Corbett, J. D. *Inorg. Chem.* **1972**, *11*, 357.
(31) Lassigne, C. R.; Wells, E. J. *J. Chem. Soc., Chem. Commun.* **1978**, 956.
(32) Schrobilgen, G. J.; Burns, R. C.; Granger, P. *J. Chem. Soc., Chem. Commun.* **1978**, 957.
(33) Burns, R. C.; Chan, W.-L.; Gillespie, R. J.; Luk, W.-C.; Sawyer, J. F.; Slim, D. R. *Inorg. Chem.* **1980**, *19*, 1432.
(34) Pyykkö, P. *Chem. Phys.* **1977**, *22*, 289.

Table II. ^{119}Sn–^{117}Sn Coupling Constants[a] for $Sn_{9-x-y}A_xB_y{}^{q-}$ Clusters

	cation				
cluster	Li	Na	K	Rb	Cs
$Sn_9{}^{4-}$	273	256	263	268	293
Sn_8Pb^{4-}	288	262	275	282	303
$Sn_7Pb_2{}^{4-}$		281	293	301	325
$Sn_6Pb_3{}^{4-}$		317	323	340	369
$Sn_5Pb_4{}^{4-}$		366	378	393	418
$Sn_4Pb_5{}^{4-}$		427	455	469	534
$Sn_3Pb_6{}^{4-}$		520		584	610
$Sn_2Pb_7{}^{4-}$				717	753
Sn_8Ge^{4-}		258	268	275	
$Sn_7Ge_2{}^{4-}$		264	278	284	
$Sn_6Ge_3{}^{4-}$		298	309	317	
$Sn_5Ge_4{}^{4-}$		394	412	416	
$Sn_4Ge_5{}^{4-}$		494	518	518	
$Sn_3Ge_6{}^{4-}$		682	713	726	
$Sn_2Ge_7{}^{4-}$			747		
Sn_8Tl^{5-}		412	456		
Sn_7PbTl^{5-}		418			
$Sn_6Pb_2Tl^{5-}$		444			
$Sn_2Bi_2{}^{2-}$	1606	1638	1638		

[a] In Hz.

Table III. ^{119}Sn–^{207}Pb Coupling Constants[a] for $Sn_{9-x-y}Pb_xTl_y{}^{8-}$ Clusters

	cation				
cluster	Li	Na	K	Rb	Cs
Sn_8Pb^{4-}	461	555	550	542	513
$Sn_7Pb_2{}^{4-}$		562	557	546	520
$Sn_6Pb_3{}^{4-}$		568	557	546	520
$Sn_5Pb_4{}^{4-}$		572	557	546	517
$Sn_4Pb_5{}^{4-}$		568	550	542	505
$Sn_3Pb_6{}^{4-}$		562	542	526	494
$Sn_2Pb_7{}^{4-}$		537	521	504	462
$SnPb_8{}^{4-}$		488	488	473	429
Sn_7PbTl^{5-}		335			
$Sn_6Pb_2Tl^{5-}$		366			

[a] In Hz.

^{119}Sn–^{203,205}Tl. (The magnetic moments of ^{203}Tl and ^{205}Tl differ by only 0.98% so that separate couplings are not resolved. We subsequently shall use the symbol Tl to refer to the mixture ^{203,205}Tl.)

Data from the ^{205}Tl spectrum of the same solution (Figure 2) confirm the assignment of cluster composition. The ratio of the height of the central peak to that of the first pair of satellites is 1:0.35:0.38, while the expected[5] intensity ratio for a cluster with eight Sn atoms and one Tl atom is 1:0.340:0.375. The ratio 0.340:0.375 is simply the ^{117}Sn/^{119}Sn ratio of 0.906. If there were seven or nine Sn's in the cluster, the expected intensities would be 1:0.306:0.334 or 1:0.373:0.410, respectively. A seven-Sn cluster is clearly ruled out by the data, while a nine-Sn cluster is a possible but poorer fit than an eight-Sn cluster. The coupling constants are 795 Hz for ^{205}Tl–^{119}Sn and 760 Hz for ^{205}Tl–^{117}Sn, the former being identical within the experimental uncertainty of ±5 Hz with that (800 Hz) measured from the ^{119}Sn spectrum.

Further evidence for the identification of Sn_8Tl^{5-}, including its charge, is given by the elemental analysis of the solid residue obtained by evaporation of the en solution. This residue has the composition $Na_5Sn_8Tl{\cdot}1.25en$ (observed percents of 2.02, 0.72, 2.68, 8.26, 71.21, and 14.57 for C, H, N, Na, Sn, and Tl vs. calculated percents of 2.23, 0.75, 2.61, 8.55, 70.65, and 15.21, respectively). The observed composition corresponds to Na:Sn:Tl mole ratios of 5.04:8.42:1.00, indicating Sn in excess of that expected for Na_5Sn_8Tl. Indeed, the solution from which the residue was obtained does exhibit a weak $Sn_9{}^{4-}$ pattern. A mixture of Na_3Sn_8Tl and Na_4Sn_9 giving an effective Na:Tl ratio of 5 would have a Sn:Tl ratio of 12.5, greatly in excess of that observed. Thus, the analysis supports the charge assignment Sn_8Tl^{5-}, although we remain open to the possibility that this cluster, as well as the Pb-substituted clusters described below, are actually of 3– charge.

Table IV. ^{119}Sn–Tl Coupling Constants[a] for $Sn_{9-x-y}Pb_xTl_y{}^{5-}$ Clusters

	cation			cation	
cluster	Na	K	cluster	Na	K
Sn_8Tl^{5-}	800 795[b]	646	$Sn_6Pb_2Tl^{5-}$	781	644
			$Sn_5Pb_3Tl^{5-}$		593
Sn_7PbTl^{5-}	791	665	$Sn_4Pb_4Tl^{5-}$		519

[a] In Hz from ^{119}Sn NMR except as noted. Tl denotes ^{203,205}Tl mixture. [b] From ^{205}Tl NMR; coupling constant for ^{205}Tl–^{117}Sn is 760 Hz.

Table V. ^{119}Sn Chemical Shifts[a] for $Sn_{9-x-y}A_xB_y{}^{q-}$ Clusters

	cation				
cluster	Li	Na	K	Rb	Cs
$Sn_9{}^{4-}$	−1241	−1230[b]	−1210	−1190	−1115
Sn_8Pb^{4-}	−1281	−1272	−1251	−1231	−1152
$Sn_7Pb_2{}^{4-}$		−1319	−1298	−1276	−1194
$Sn_6Pb_3{}^{4-}$		−1366	−1344	−1321	−1235
$Sn_5Pb_4{}^{4-}$		−1420	−1397	−1373	−1281
$Sn_4Pb_5{}^{4-}$		−1480	−1456	−1430	−1333
$Sn_3Pb_6{}^{4-}$		−1538	−1512	−1484	−1381
$Sn_2Pb_7{}^{4-}$		−1579	−1553	−1523	−1414
$SnPb_8{}^{4-}$		−1610	−1587	−1554	−1438
Sn_8Ge^{4-}		−1223	−1204	−1183	
$Sn_7Ge_2{}^{4-}$		−1201	−1192	−1161	
$Sn_6Ge_3{}^{4-}$		−1185	−1167	−1145	
$Sn_5Ge_4{}^{4-}$		−1180	−1161	−1139	
$Sn_4Ge_5{}^{4-}$		−1187	−1168	−1145	
$Sn_3Ge_6{}^{4-}$		−1188	−1167	−1144	
$Sn_2Ge_7{}^{4-}$		−1202	−1178	−1154	
$SnGe_8{}^{4-}$		−1237	−1214		
Sn_8Tl^{5-}		−1169	−1137		
Sn_7PbTl^{5-}		−1218	−1183		
$Sn_6Pb_2Tl^{5-}$		−1266	−1227		
$Sn_5Pb_3Tl^{5}$			−1270		
$Sn_4Pb_4Tl^{5-}$			−1317		
$Sn_2Bi_2{}^{2-}$		−1674	−1575		

[a] Chemical shifts δ relative to Me_4Sn external. [b] δ −1253 with 2,2,2-crypt present.

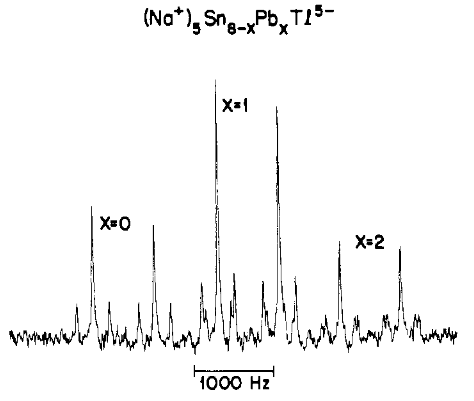

Figure 3. NMR spectrum of ^{119}Sn at 33.4 MHz for $(Na^+)_5Sn_{8-x}Pb_xTl^{5-}$ in en, showing regions corresponding to x = 0–2.

Spectra of ^{119}Sn similar to that in Figure 1 have been obtained from en solutions of the ternary alloy $K_2Sn_2Tl_3$ and quaternary alloys $Na_2SnPbTl_3$ and $K_2SnPbTl_3$. While the cluster Sn_8Tl^{5-} is identified from the spectrum of the $K_2Sn_2Tl_3$ solution, with parameters (Tables II–V) very similar to those for the $Na_2Sn_2Tl_3$ solution, a new series of clusters, namely $Sn_{8-x}Pb_xTl^{5-}$ (x = 1–4) are identified from the spectra of solutions of the quaternary alloys. The spectra of the various series members are characterized by ^{119}Sn chemical shift differences resembling those we previously reported[4] for the series $Sn_{9-x}Pb_x{}^{4-}$, namely shifts to high field of approximately 50 ppm (Table V) for each Pb atom replacing an Sn atom. We have identified ternary clusters $Sn_{8-x}Pb_xTl^{5-}$ with x = 1, 2 for Na^+ and with x = 1–4 for K^+. The spectra for a given cation are adequately separated for various x values (Figure 3, for Na^+ with x = 0. 1, and 2) and may be identified as to the number of Sn atoms in the usual manner[4-6] (Figure 4, for Na^+ with x = 1). The signal-to-noise ratio for these spectra is not

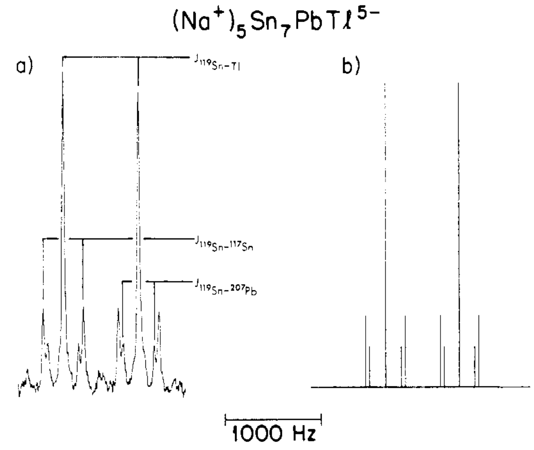

Figure 4. (a) Detail from Figure 3 for Sn_7PbTl^{5-}. (b) Line spectrum calculated with $J(^{119}Sn-^{117}Sn)$ = 418 Hz, $J(^{119}Sn-^{203,205}Tl)$ = 791 Hz, and $J(^{119}Sn-^{207}Pb)$ = 335 Hz. Comparison of expected intensities to peak heights is given in text.

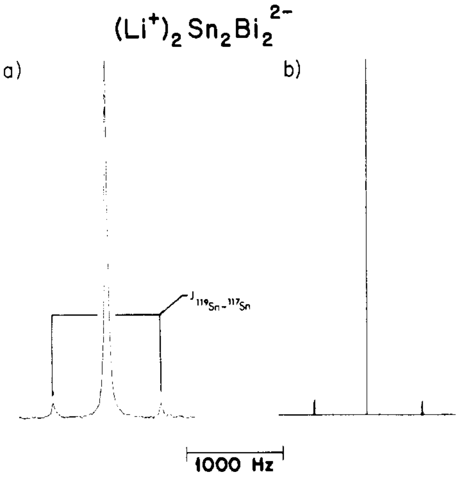

Figure 5. (a) NMR spectrum of ^{119}Sn at 134.0 Hz for $(Li^+)_2Sn_2Bi_2^{2-}$ in en. (b) Line spectrum calculated for $Sn_2Bi_2^{2-}$ with $J(^{119}Sn-^{117}Sn)$ = 1606 Hz. The observed ratio of central to satellite peak heights in (a) is 1:0.037 while the expected intensity for a cluster with two Sn atoms is 1:0.041.

nearly as large as that for Sn_8Tl^{5-} in Figure 1 but appears to be sufficient for establishing cluster compositions. For Sn_7PbTl^{5-} (Figure 4), the observed peak height ratios are 1.00:0.26:0.14 with an uncertainty of ±4–5%, while the expected intensity ratios for a seven-Sn cluster are 1.00:0.236:0.136. The various coupling constants for ^{119}Sn to ^{117}Sn, Tl, and ^{207}Pb are listed in Tables II–IV. No confirmation for the assignment of the charge −5 to these clusters has been obtained, except that we note that the ^{119}Sn chemical shifts (Table V) are in line with that for Sn_8Tl^{5-} (chemical analysis of solid residue quoted above), so that it is probable that the $Sn_{8-x}Pb_xTl^{5-}$ clusters have the same charge as Sn_8Tl^{5-}.

C. $Sn_2Bi_2^{2-}$. The anion $Sn_2Bi_2^{2-}$ has been identified[18] by X-ray diffraction of crystals of $(2,2,2\text{-crypt-}K^+)_2Sn_2Bi_2^{2-}\cdot en$. We report here the ^{119}Sn NMR identification of this anion in en solution. Solutions of the alloy LiSnBi exhibit only the two-Sn pattern (Figure 5a) with a large upfield shift of −1674 ppm, which we assign to $Sn_2Bi_2^{2-}$. The observed ratio of the central to the satellite peak heights is 1:0.037 while the expected intensity ratio (Figure 5b) is 1:0.041. For a three-Sn cluster the ratio would be 1:0.082, enough different so that the low satellite intensity does not preclude determination of the number of Sn atoms in the cluster. The solid residue obtained by evaporation was found to have a composition $Li_2Sn_2Bi_2\cdot 3.2en$ (observed percents of 9.47, 3.21, 11.03, 1.55, 29.39, and 44.87 for C, H, N, Li, Sn, and Bi vs. calculated percents of 9.60, 3.22, 11.20, 1.58, 26.95, and 47.75, respectively). Admittedly, this analysis presents some difficulties, as the observed composition has a lower Bi/Sn ratio than that calculated. Nevertheless, the large upfield shift strongly suggests a cluster with a greater negative charge per Sn atom than that in any of the nine-atom clusters. Indeed, the shift is comparable to the −1895 ppm value we earlier[6] assigned to Sn_4^{2-}.

Table VI. ^{207}Pb Chemical Shifts[a] for $Sn_{9-x}Pb_x^{4-}$ Clusters

	cation				
cluster	Li	Na	K	Rb	Cs
Pb_9^{4-}	−1224	−1189	−1137	−1061	−819
$SnPb_8^{4-}$		−971	−950	−877	−648
$Sn_2Pb_7^{4-}$		−770	−756	−687	−469
$Sn_3Pb_6^{4-}$		−573	−556	−491	−284
$Sn_4Pb_5^{4-}$		−382	−366	−303	−104
$Sn_5Pb_4^{4-}$		−207	−191	−130	+62
$Sn_6Pb_3^{4-}$		−40	−24	+35	+221
$Sn_7Pb_2^{4-}$		+136	+153	+210	+376
Sn_8Pb^{4-}		+294	+311	+367	

[a] Chemical shifts δ relative to 1 M $Pb(NO_3)_2$, external.

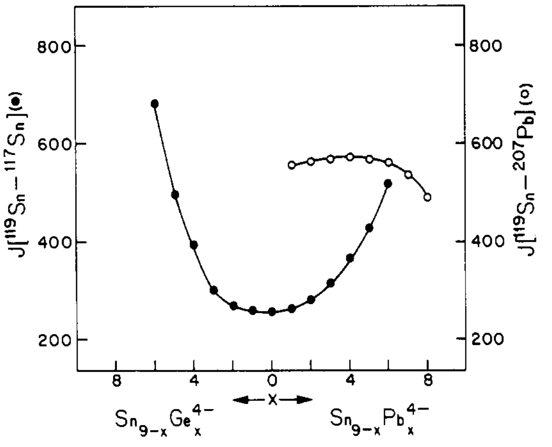

Figure 6. Spin–spin coupling constants *J* in Hz vs. *x* for $^{119}Sn-^{117}Sn$ (●) for the series $Sn_{9-x}Ge_x^{4-}$ and $Sn_{9-x}Pb_x^{4-}$; coupling constants *J* in Hz vs. *x* for $^{119}Sn-^{207}Pb$ (○) for the series $Sn_{9-x}Pb_x^{4-}$. All data are for Na^+ solutions in en (see Tables II and III).

Solutions of NaSnBi exhibit not only the pattern attributable to $Sn_2Bi_2^{2-}$, as with solutions of LiSnBi, but also an eight-Sn pattern with $\delta(^{119}Sn)$ very close to that of Sn_9^{4-} (−1231 vs. −1230 ppm). Our tentative identification of this pattern is that it arises from Sn_8Bi^{3-}, just as an eight-Sn pattern seen in solutions of various Na–Sn–Sb alloys[4] was associated with Sn_8Sb^{3-}. However, as we do not have a confirmation of either the number of "heteroatoms" (Bi or Sb) in these clusters or the charge, we do not include their spectral parameters in our present tabulations.

IV. NMR Parameters

In this section we present and discuss a compilation of coupling constants and chemical shifts not only for the clusters described in Section III but also for the previously reported clusters $Sn_{9-x}M_x^{4-}$ (M = Pb, Ge; x = 0–8). Data for the latter clusters were previously reported for Na^+ only; here we present data for Li^+, K^+, Rb^+, and Cs^+ solutions in en as well. Table II gives $^{119}Sn-^{117}Sn$ coupling constants; Table III, $^{119}Sn-^{207}Pb$ coupling constants; Table IV, ^{119}Sn–Tl coupling constants; Table V, ^{119}Sn chemical shifts; and Table VI, ^{207}Pb chemical shifts.

Many systematic trends may be noted from the NMR parameters given in Tables II–VI and Figures 6–8. These trends include the following:

(a) The couplings $J(^{119}Sn-^{117}Sn)$ for both $Sn_{9-x}Pb_x^{4-}$ and $Sn_{9-x}Ge_x^{4-}$ have an approximately parabolic dependence (Table II and Figure 6) on *x*, with *J* increasing 100 to 175% in going from Sn_9^{4-} to $Sn_3M_6^{4-}$ (M = Pb, Ge) and about 250% in going to $Sn_2Ge_7^{4-}$. The simplest explanation of this dependence is an increasing tendency toward Sn–Sn association with increasing *x*. In a later section we discuss the results of our calculations of *J* for representative clusters, with emphasis on the difference in *J* for neighboring vs. nonneighboring Sn–Sn pairs.

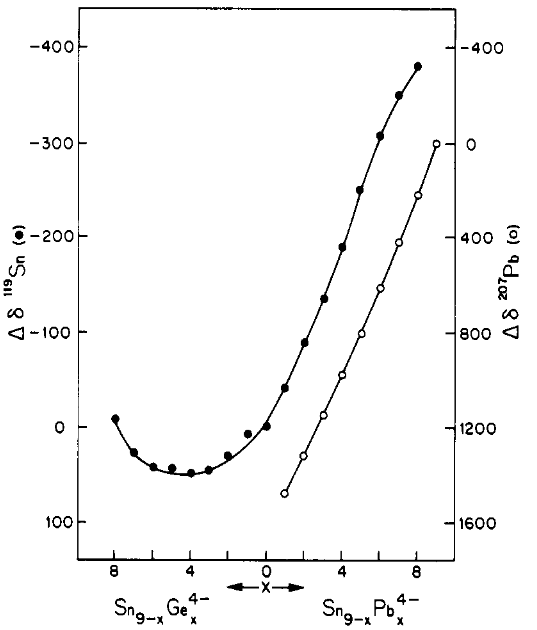

Figure 7. Chemical shifts δ vs. x for ^{119}Sn (●) for the series $Sn_{9-x}Ge_x^{4-}$ and $Sn_{9-x}Pb_x^{4-}$; chemical shifts δ in ppm vs. x for ^{207}Pb (○) for series $Sn_{9-x}Pb_x^{4-}$. All data are for Na^+ solutions in en. The ^{119}Sn δ value for Sn_9^{4-} and the ^{207}Pb value for Pb_9^{4-} are each taken as zero (see Tables V and VI).

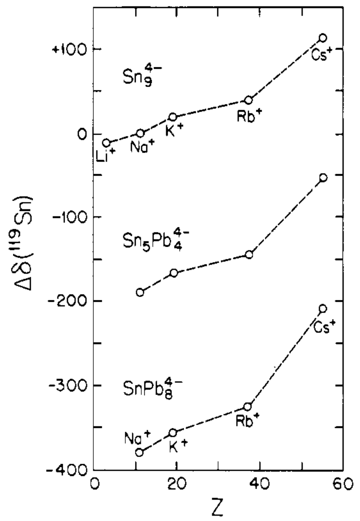

Figure 8. Plot of the ^{119}Sn chemical shift δ for solutions in en of Sn_9^{4-}, $Sn_5Pb_4^{4-}$, and $SnPb_8^{4-}$ vs. the atomic number Z of the accompanying alkali-metal cation. The δ value for ($4Na^+$, Sn_9^{4-}) is taken as zero (see Table V).

(b) The couplings $J(^{119}Sn-^{207}Pb)$ are nearly independent of x for the series $Sn_{9-x}Pb_x^{4-}$ but do decrease slightly for large x (Table II and Figure 6). Note that any clustering (segregation) of Pb atoms, e.g. for $x = 2$ or 3, should not significantly affect the Sn–Pb couplings as compared to those for $x = 1$. If, however, alkali metals strengthen the segregation, they shorten the average Sn–Sn distance and lengthen the average Sn–Pb (or Sn–Tl) distances; the trends are coherent.

(c) The couplings $J(^{119}Sn-^{117}Sn)$ are somewhat dependent on the cation (Table I), increasing typically 50 Hz in going from Na^+ to Cs^+. The $J(^{119}Sn-^{207}Pb)$ and $J(^{119}Sn-Tl)$ values (Tables II and III) decrease slightly with increasing Z at the cation.

(d) The steep and roughly linear variation of $\delta(^{119}Sn)$ with x for the series $Sn_{9-x}Pb_x^{4-}$, with a shift to more negative δ (upfield) by approximately 60 ppm/Pb atom replacing a Sn atom, has been previously reported[4,5] for solutions containing Na^+ and discussed[35] by L.L.L. in terms of charge distributions and electronegativity equalization. The "heavy-atom" effect[36] could also be invoked, but as the relativistic theory of the NMR chemical shift[37] has not yet been implemented as a working procedure, no definite conclusions can be drawn. We do note, however, that the shifts to high field of δ(Sn) and δ(Pb) for $Sn_{9-x}Pb_x^{4-}$ follow the normal trend[37a] for heavy-atom substituents.[8] In Table V we present data showing the variations of δ with x as a function of the alkali-metal cation. The effect is essentially the same for each alkali metal as that shown in Figure 3 for Na^+.

(e) As in part d, the previously noted[6] approximate independence (±25 ppm) of $\delta(^{119}Sn)$ on x for the series $Sn_{9-x}Ge_x^{4-}$ holds for all of the cations studied (Table V and Figure 7). The changes are much smaller for Ge than for Pb, supporting the idea of a heavy-atom effect for the latter substitution.

(f) Again as in part d, the previously noted[4] steep and nearly linear dependence of $\delta(^{207}Pb)$ with x, corresponding to an upfield shift of approximately 200 ppm/Pb atom replacing a Sn atom, holds for all of the cations studied (Table VI and Figure 7).

(g) For a given member of the $Sn_{9-x}Pb_x^{4-}$ series, $\delta(^{119}Sn)$ becomes less negative (downfield) by approximately 140 ppm in going from Na^+ to Cs^+, with this cation dependence (Table V) being somewhat less (115 ppm) for $x = 0$ and somewhat larger (172 ppm) for $x = 8$. In Figure 8 we show this dependence for three members of $Sn_{9-x}Pb_x^{4-}$, namely for $x = 0$, 4, and 8. The effect on δ of replacing Na^+ by Cs^+ for a given anion is approximately the same in magnitude but opposite in sign to that of replacing three Sn atoms by three Pb atoms for a given cation, namely a change in δ of approximately 120–160 ppm. The cation effect may simply reflect a greater degree of cation–anion association with Cs^+ than with Li^+ or Na^+ (reduced cation complexation by en). Figure 8 also shows that the variation of $\delta(^{119}Sn)$ with x as described in part d above is essentially identical for each cation studied.

(h) Similarly, $\delta(^{207}Pb)$ for this series becomes more positive (downfield) by approximately 300 ppm in going from Na^+ to Cs^+ (Table V), again with a smaller change (240 ppm) for small x ($x = 2$) and a larger change (370 ppm) for large x ($x = 9$). This variation, as well as the similar variation of $\delta(^{119}Sn)$ with the nature of the cation as described in part g, may be concentration-dependent, although no appreciable concentration dependence of $\delta(^{119}Sn)$ was detected (±20 Hz at 34 kHz, or less than 1 ppm) for Sn_9^{4-} with Na^+ over the cluster concentration range of 10^{-4}–0.01 M.

Our solutions, which are typically 0.01–0.1 M with respect to the anionic cluster, were prepared with excess alloy in contact with the solvent en for 2–24 h, in general, and 48 h–2 weeks for alloys containing Na. Thus, the solutions contain the maximum concentration of clusters extractable at room temperature. The order of solubilities for $(M^+)_4Sn_9^{4-}$ in en is $Li^+ < Na^+ < K^+ \sim Rb^+ > Cs^+$. The maximum concentration achieved is approximately 0.05 M with respect to the cluster for Rb^+, while for Li^+ and Cs^+ the solubilities are approximately 0.01 M.

The dependences of chemical shifts of certain other anions not only on the nature of the cation but also on the electrolyte concentration are well established,[38-40] as are similar dependences of cation shifts on the nature of the anion.[38-41] For example, the ^{35}Cl δ values in aqueous alkali-metal chloride solutions[38,39] are

---

(35) Lohr, L. L. *Int. J. Quantum Chem.* **1984**, *25*, 211.

(36) (a) Nomura, Y.; Takeuchi, Y.; Nakagawa, N. *Tetrahedron Lett.* **1969**, *10*, 639. (b) Cheremisin, A. A.; Schastnev, P. V. *J. Magn. Reson.* **1980**, *40*, 459. (c) Morishima, I.; Endo, K.; Yonezawa, T. *J. Chem. Phys.* **1973**, *59*, 3356. (d) Kidd, R. G. *Annu. Rep. NMR Spectrosc.* **1980**, *10A*, 1.

(37) (a) Pyykkö, P. *Chem. Phys.* **1983**, *74*, 1. (b) Pyper, N. C. *Chem. Phys. Lett.* **1983**, *96*, 204. (c) Zhang, Z. C.; Webb, G. A. *J. Mol. Struct.* **1983**, *104*, 439.

(38) Deverell, C.; Richards, R. E. *Mol. Phys.* **1966**, *10*, 551.

(39) Deverell, C. *Progress in Nuclear Magnetic Resonance Spectroscopy*; Emsley, J. W., Feeney, J., Sutcliffe, L. H., Eds.; Pergamon: Oxford, 1969; Vol. 4, pp 235–334.

(40) Lindman, B.; Forsén, S. *NMR and the Periodic Table*; Harris, R. K., Mann, B. E., Eds.; Academic: London, 1978; pp 129–181.

(41) Shih, J. S.; Popov, A. I. *Inorg. Nucl. Chem. Lett.* **1977**, *13*, 105.

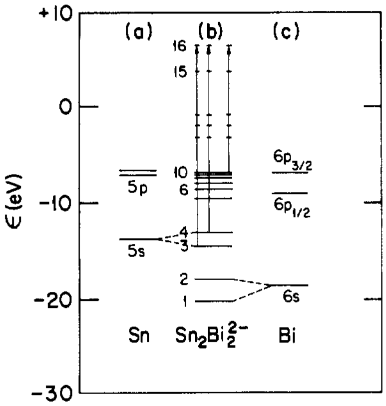

Figure 9. Orbital energies in eV computed at the REX level for $Sn_2Bi_2^{2-}$, C_{2v} symmetry. The input atomic energy parameters are shown on the left (a) for Sn and on the right (c) for Bi. Arrows indicate the excitations giving the largest computed contributions to $J(^{119}Sn-^{117}Sn)$.

increasingly to low field for the series Na^+, K^+, Rb^+, and Cs^+. The concentration dependence is also greatest for Cs^+, being approximately 4 ppm m^{-1} (to lower fields), with the dependences for the other cations being significantly less.

V. Origin of the Spin–Spin Couplings

In order to understand better the origin of the spin–spin couplings in these heavy-element clusters, we carried out calculations of the coupling tensors for several representative clusters by using the relativistically parametrized extended Hückel (REX) approach,[42,43] which has been previously used in implementations[44,45] of the relativistic theory[34] of nuclear spin–spin couplings. We have previously applied the REX method[46] to a large number of these main-group anionic and cationic clusters, in a study similar to a nonrelativistic study[47] of the electronic structures of clusters.

As a first example we consider the cluster $Sn_2Bi_2^{2-}$, characterized in solution (Na^+ in en) by $J(^{119}Sn-^{117}Sn) = 1638$ Hz and $\delta(^{119}Sn)$ -1674 ppm relative to Me_4Sn. In the solid (2,2,2-crypt-K)$_2$Sn$_2$Bi$_2$, the cluster has a nearly tetrahedral structure,[18] with all edges close to the 2.96 Å average edge length. Assuming an idealized tetrahedral structure (symmetry C_{2v}) with all edges exactly 2.95 Å, we obtain the REX orbital energy levels shown in Figure 9. The arrows indicate the excitations with particularly large contributions to the spin–spin coupling. Although there is only one irreducible representation (Γ_5 or $e_{1/2}$) for the double-group C_{2v}^*, the MO's of $Sn_2Bi_2^{2-}$ do retain a recognizable identity in terms of the group C_{2v}. For example, MO's 3 and 4, at -14.5 and -13.2 eV, respectively, comprise a Sn(5s) "band", with symmetric (a_1) and antisymmetric (b_1) combinations of the Sn(5s) AO's predominating in these MO's. Specifically, the percentage of Sn(5s) character in these MO's is 37.4 and 38.4% per Sn atom, respectively. Excitations from these MO's to MO(16), the highest virtual MO, give large but opposite contributions to the spin–spin coupling constant of +21.0 and -26.8 kHz, respectively. This MO(16) has percentages per Sn atom of 8.6, 7.5, and 26.7 for 5s, $5p_{1/2}$, and $5p_{3/2}$, respectively. The most important remaining contribution (8.5 kHz) is the excitation from the HOMO(10) at -7.1 eV to MO(16); the HOMO is also predominantly Sn in character, with percentages per Sn atom of 1.9, 23.9, and 14.3 for 5s, $5p_{1/2}$, and $5p_{3/2}$, respectively. The sum of all isotropic contributions is +1137 Hz, roughly comparable, given the crude nature of the calculations, to the observed value of ±1638 Hz if the latter is positive in sign. Although we have computed the individual components, including the anisotropic J_{yz} component of a coupling tensor with principal axes x, y, and z parallel to the Sn–Sn, the Bi–Bi, and the cluster C_2 axes, respectively, we do not report these details, but simply note the order $J_{yy} > J_{zz} > J_{xx}$, with J_{yy} approximately twice J_{xx}.

The origin of these isotropic coupling constants resembles that in certain lead organometallic compounds,[45] where the deep-lying MO's with Pb 6s gave large but nearly canceling contributions; the large observed variations of the Pb–Pb and Pb–C couplings from compound to compound were attributed to changes in the frontier MO, which has some Pb 6s character. Adding to these inner cancellations at a given geometry the computational difficulties arising from the fluxionality, we omit the detailed values we calculated for Sn_4^{2-}, Sn_5^{2-}, Sn_9^{4-}, and Sn_8Pb^{4-}. We note that for clusters with a large HOMO–LUMO gap, e.g. 3 eV or greater, the isotropic couplings are dominated by the "contact", or s-type AO, contributions. However, for Sn_4^{2-}, with a HOMO–LUMO gap at the REX level of only 1.6 eV, the coupling constant computed at the same compressed D_{2d} geometry (Sn–Sn = 3.11 and 3.77 Å) that we obtained[48] by energy minimization at the nonrelativistic effective potential level has important noncontact contributions. Finally, we note that adjacent Sn atoms in clusters such as Sn_4^{2-} typically have computed isotropic $J(^{119}Sn-^{117}Sn)$ values in the range of -500 to -1200 Hz, while for nonadjacent atoms the values are typically +300 to +800 Hz. Thus, a proper calculation for a fluxional molecule would involve a hierarchy of averagings with extensive cancellations at every level: the summations over occupied and unoccupied MO's for a given pair in a given structure, the averaging over pairs in a given structure, and the averaging over thermally accessible structures. The semiquantitative accuracy of our present method does not justify such an exercise.

VI. Summary

Anionic clusters of the elements Ge, Sn, Sb, Tl, Pb, and Bi have been generated by dissolving alkali-metal alloys in liquid ethylenediamine. The clusters have been identified by ^{119}Sn and ^{207}Pb NMR techniques. Spin–spin coupling constants ($^{119}Sn-^{117}Sn$, $^{119}Sn-Tl$, and $^{119}Sn-^{207}Pb$) and chemical shifts (^{119}Sn and ^{207}Pb) are presented for a large number of clusters with alkali-metal cations ranging from Li^+ to Cs^+. Clusters not previously reported include $Sn_{8-x}Pb_xTl^{5-}$ (x = 1–4); $Sn_2Bi_2^{2-}$, for which a crystal structure is known,[18] is characterized by NMR for the first time. A number of systematic trends in the data are presented and discussed. For the series $Sn_{9-x}Ge_x^{4-}$ and $Sn_{9-x}Pb_x^{4-}$ there are significant and nearly quadratic increases in $J(^{119}Sn-^{117}Sn)$ as x goes from 0 (all Sn) to 7 (two Sn atoms per cluster). The increases, of approximately 250%, are probably indicative of a tendency toward Sn–Sn association within the heteronuclear clusters. Dependencies of the ^{119}Sn and ^{207}Pb chemical shifts on the nature of the alkali-metal cation are also discussed. Finally, the origins of the spin–spin couplings are discussed in terms of the relativistic theory of the coupling as implemented with the relativistically parametrized extended Hückel (REX) method. Large "contact" contributions to the isotropic coupling constant are found to arise from excitations from the mostly Sn(5s) MO's; these contributions tend to cancel when summed over the occupied MO's. Important but highly variable contributions are also associated with the Sn(5s) character of the frontier orbital (HOMO). In conclusion, the various results indicate the power of multinuclear NMR techniques in identifying and characterizing main-group anionic clusters.[50]

---

(42) Lohr, L. L.; Pyykkö, P. *Chem. Phys. Lett.* **1979**, *62*, 333.
(43) Lohr, L. L.; Hotokka, M.; Pyykkö, P. *QCPE* **1980**, *12*, 387.
(44) Pyykkö, P.; Wiesenfeld, L. *Mol. Phys.* **1981**, *43*, 557.
(45) Pyykkö, P. *J. Organomet. Chem.* **1982**, *232*, 21.
(46) Lohr, L. L. *Inorg. Chem.* **1981**, *20*, 4229.
(47) Burns, R. C.; Gillespie, R. J.; Barnes, J. A.; McGlinchey, M. J. *Inorg. Chem.* **1982**, *21*, 799.
(48) Rothman, M. J.; Bartell, L. S.; Lohr, L. L. *J. Am. Chem. Soc.* **1981**, *103*, 2482.
(49) The periodic group notation in parentheses is in accord with recent actions by IUPAC and ACS nomenclature committees. A and B notation is eliminated because of wide confusion. Groups IA and IIA become groups 1 and 2. The d-transition elements comprise groups 3 through 12, and the p-block elements comprise groups 13 through 18. (Note that the former Roman number designation is preserved in the last digit of the new numbering: e.g., III → 3 and 13.)
(50) For a recent application of multinuclear techniques to anions of Cd, Sn, Hg, or Tl with Se or Te, see: Burns, R. C.; Devereux, L. A.; Granger, P.; Schrobilgen, G. J. *Inorg. Chem.* **1985**, *24*, 2615.

Inorg. Chem. **1986**, *25*, 1541–1546 **1541**

Acknowledgment. We thank Dr. Melvin L. Luetkens, Jr., of the University of Michigan for many helpful suggestions. We thank the NSF for partial support of this work and for funds for the purchase of a FT-NMR spectrometer under Grant CHE76-23334. L.L.L. wishes to thank the Academy of Finland for funds used in support of his visit to the University of Helsinki in July 1984, during which time this paper was completed.

Registry No. Li_4Sn_9, 101419-04-9; Na_4Sn_9, 12533-62-9; K_4Sn_9, 84109-35-3; Rb_4Sn_9, 101419-05-0; Cs_4Sn_9, 101419-06-1; Li_4Sn_8Pb, 101419-07-2; Na_4Sn_8Pb, 101419-08-3; K_4Sn_8Pb, 101419-09-4; Rb_4Sn_8Pb, 101419-10-7; Cs_4Sn_8Pb, 101419-11-8; $Na_4Sn_7Pb_2$, 101419-12-9; $K_4Sn_7Pb_2$, 101419-13-0; $Rb_4Sn_7Pb_2$, 101419-14-1; $Cs_4Sn_7Pb_2$, 101419-15-2; $Na_4Sn_6Pb_3$, 101419-16-3; $K_4Sn_6Pb_3$, 101419-17-4; $Rb_4Sn_6Pb_3$, 101419-18-5; $Cs_4Sn_6Pb_3$, 101419-19-6; $Na_4Sn_5Pb_4$, 101419-20-9; $K_4Sn_5Pb_4$, 101419-21-0; $Rb_4Sn_5Pb_4$, 101419-22-1; $Cs_4Sn_5Pb_4$, 101419-23-2; $Na_4Sn_4Pb_5$, 101419-24-3; $K_4Sn_4Pb_5$, 101419-25-4; $Rb_4Sn_4Pb_5$, 101419-26-5; $Cs_4Sn_4Pb_5$, 101419-27-6; $Na_4Sn_3Pb_6$, 101419-28-7; $K_4Sn_3Pb_6$, 101419-29-8; $Rb_4Sn_3Pb_6$, 101419-30-1; $Cs_4Sn_3Pb_6$, 101419-31-2; $Na_4Sn_2Pb_7$, 101419-32-3; $K_4Sn_2Pb_7$, 101419-33-4; $Rb_4Sn_2Pb_7$, 101419-34-5; $Cs_4Sn_2Pb_7$, 101470-92-2; Na_4SnPb_8, 101419-35-6; K_4SnPb_8, 101419-36-7; Rb_4SnPb_8, 101419-37-8; Cs_4SnPb_8, 101419-38-9; Na_4Sn_8Ge, 101419-39-0; K_4Sn_8Ge, 101419-40-3; Rb_4Sn_8Ge, 101470-93-3; $Na_4Sn_7Ge_2$, 101419-41-4; $K_4Sn_7Ge_2$, 101419-42-5; $Rb_4Sn_7Ge_2$, 101470-94-4; $Na_4Sn_6Ge_3$, 101419-43-6; $K_4Sn_6Ge_3$, 101419-44-7; $Rb_4Sn_6Ge_3$, 101419-45-8; $Na_4Sn_5Ge_4$, 101419-46-9; $K_4Sn_5Ge_4$, 101419-47-0; $Rb_4Sn_5Ge_4$, 101470-95-5; $Na_4Sn_4Ge_5$, 101419-48-1; $K_4Sn_4Ge_5$, 101419-49-2; $Rb_4Sn_4Ge_5$, 101419-50-5; $Na_4Sn_3Ge_6$, 101419-51-6; $K_4Sn_3Ge_6$, 101419-52-7; $Rb_4Sn_3Ge_6$, 101419-53-8; $Na_4Sn_2Ge_7$, 101419-54-9; $K_4Sn_2Ge_7$, 101470-96-6; $Rb_4Sn_2Ge_7$, 101419-55-0; Na_4SnGe_8, 101419-56-1; K_4SnGe_8, 101419-57-2; Na_5Sn_8Tl, 89680-10-4; K_5Sn_8Tl, 101419-58-3; Na_5Sn_7PbTl, 101419-59-4; K_5Sn_7PbTl, 101419-60-7; $Na_5Sn_6Pb_2Tl$, 101419-61-8; $K_5Sn_6Pb_2Tl$, 101419-62-9; $K_5Sn_5Pb_3Tl$, 101419-63-0; $K_5Sn_4Pb_4Tl$, 101419-64-1; $Na_2Sn_2Bi_2$, 101419-65-2; $K_2Sn_2Bi_2$, 82150-33-2; Li_4Pb_9, 101419-66-3; Na_4Pb_9, 101419-67-4; K_4Pb_9, 84109-36-4; Rb_4Pb_9, 101419-68-5; Cs_4Pb_9, 101419-69-6; ^{119}Sn, 14314-35-3; ^{205}Tl, 14280-49-0; ^{207}Pb, 14119-29-0; ^{117}Sn, 13981-59-4; ^{203}Tl, 14280-48-9.

Contribution from the Department of Synthetic Chemistry,
Kyoto University, Sakyo-ku Yoshida, Kyoto, 606 Japan

Kinetic Investigation of Uranyl–Uranophile Complexation. 1. Macrocyclic Kinetic Effect and Macrocyclic Protection Effect

Iwao Tabushi* and Atsushi Yoshizawa

Received May 7, 1985

Equilibria and rates of ligand-exchange reactions between uranyl tricarbonate and dithiocarbamates and between uranyl tris(dithiocarbamates) and carbonate were studied under a variety of conditions. The dithiocarbamates used were acyclic diethyldithiocarbamate and macrocyclic tris(dithiocarbamate). The acyclic ligand showed a triphasic (successive three-step) equilibrium with three different equilibrium constants while the macrocyclic ligand showed a clear monophasic (one-step) equilibrium with a much larger stability constant for the dithiocarbamate–uranyl complex. The macrocyclic ligand showed the S_N2-type ligand-exchange rate in the forward as well as reverse process, while the first step of the acyclic ligand-exchange reactions proceeded via the S_N1-type mechanism. This kinetic macrocyclic effect on molecularity is interpreted as the result of a unique topological requirement of uranyl complexation. The macrocyclic ligand also exhibited a clear protection effect, leading to the large stability constant.

Uranyl ion, UO_2^{2+} (U^{VI}), the most stable species among uranium compounds present in nature, has a linear structure[1] with a unique form of ligand coordination. According to X-ray crystallographic studies,[2] usually uranyl complexes have six ligands attached to the uranium center. These ligands are nearly on a plane (with small vertical deviation), which is perpendicular to the UO_2^{2+} ion axis. Anionic ligands are usually favored over neutral ligand complexation, thus leading to the formation of stable anionic coordination complexes. As a consequence, the most stable of all uranium derivatives are hydrophilic and highly soluble in water.

Therefore, most of the uranium on Earth is present in seawater (ca. 10^9 tons) and little is present on the land surface (ca. 10^6 tons).[3] This unusual situation prompted us to design and synthesize "uranophiles"—specific and strong ligands toward uranyl ion—in order to provide a possibility for the efficient extraction of uranyl ions from seawater.[3,5] The extraction experiments have been repeatedly carried out near the Izu Islands with promising results.[6]

Two major mechanisms for the ligand exchange of uranyl complexes—S_N1 type[7] and S_N2 type[8]—have been reported in the literature. However, no detailed discussion has ever been made about what determines the mechanism. In fact, there has been only one rate analysis of the three successive reversible processes in uranyl ligand exchange, and this analysis assumed an S_N2 mechanism without determining the rate order experimentally.[9]

This paper describes the results of detailed studies on the multistep equilibria of the ligand-exchange reactions between carbonate and the dithiocarbamates and on the kinetics of the first step of the forward as well as the reverse reaction. The macrocyclic ligand is first used for comparison with the acyclic ligand, revealing remarkable macrocyclic effects operating in this system. Noteworthy characteristics of the ligand-exchange reaction for the negatively charged macrocycles (uranophiles) are (1) a kinetic *macrocyclic molecularity effect* (the ligand-exchange mechanism is S_N2 type for the macrocycle but S_N1 type for the corresponding acylic ligand) and (2) a macrocyclic protection effect, extremely slow dissociation of macrocyclic uranyl com-

---

* To whom correspondence should be addressed.

(1) Cattalini, L.; Croatto, U.; Degetto, S.; Tondello, E. *Inorg. Chim, Acta, Rev.* **1971**, *5*, 19.
(2) Zachariasen, W. H.; Pdettinger, H. A. *Acta Crystallogr.* **1959**, *12*, 526.
(3) Tabushi, I.; Kobuke, T.; Yoshizawa, A. *J. Am. Chem. Soc.* **1984**, *106*, 2481.
(4) *Uranium Resources, Production and Demand*; NEA(OECD), Dec 1975. Uranium in land in the readily accessible state is ca. 10^6 tons.
(5) (a) Tabushi, I.; Kobuke, Y.; Nishiya, T. *Nature (London)* **1979**, *280*, 665. (b) Tabushi, I.; Kobuke, Y.; Ando, K.; Kishimoto, M.; Ohara, E. *J. Am. Chem. Soc.* **1980**, *102*, 5947.
(6) Tabushi, I.; Kobuke, Y.; Nakayama, N.; Aoki, T.; Yoshizawa, A. *Ind. & Eng. Chem. Prod. Res. Dev.* **1984**, *23*, 445.
(7) (a) Crea, J.; Diguisto, R.; Lincoln, S. F.; Williams, E. H. *Inorg. Chem.* **1977**, *16*, 2825. (b) Bowen, R. P.; Lincoln, S. F.; Williams, E. H. *Inorg. Chem.* **1976**, *15*, 2126. (c) Geoffrey, J. H.; Stephan, F. L.; Williams, E. H. *J. Chem. Soc., Dalton Trans.* **1979**, 320. (d) Bokolo, K.; Delpuech, J-J.; Rodehuser, L.; Rubini, P. R. *Inorg. Chem.* **1981**, *20*, 992. (e) Ikeda, Y.; Tomiyasu, H.; Fukutomi, H. *Bull. Chem. Soc. Jpn.* **1983**, *56*, 1060. (f) Ikeda, Y.; Tomiyasu, H.; Fukutomi, H. *Inorg. Chem.* **1984**, *23*, 3197.
(8) (a) Hurwitz, P.; Kustin, K. *J. Phys. Chem.* **1967**, *71*, 324. (b) Cattalini, L.; Vigato, P. A.; Vidali, M.; Degetto, S.; Casellato, U. *J. Inorg. Nucl. Chem.* **1975**, *37*, 1721. (c) Edstrom, A.; Johnson, D. A. *J. Inorg. Nucl. Chem.* **1974**, *36*, 2549. (d) Ishii, H.; Odashima, T.; Mogi, H. *Nippon Kagaku Kaishi* **1983**, 1422.
(9) See ref 8a.

0020-1669/86/1325-1541$01.50/0